



## Gamma-Ray Transitions Induced in Nuclear Spin Isomers by X-Rays

C. B. COLLINS<sup>1</sup>, A. C. RUSU<sup>1</sup>, N. C. ZOITA<sup>1</sup>, M. C. IOSIF<sup>1</sup>, D. T. CAMASE<sup>1</sup>,  
F. DAVANLOO<sup>1</sup>, C. A. UR<sup>2</sup>, I. I. POPESCU<sup>2</sup>, J. M. POUVESLE<sup>3</sup>,  
R. DUSSART<sup>3</sup>, V. I. KIRISCHUK<sup>4</sup>, N. V. STRILCHUK<sup>4</sup> and F. J. AGEE<sup>5</sup>

<sup>1</sup>*Center for Quantum Electronics, University of Texas at Dallas, PO Box 830688, Richardson, TX 75083-0688, USA*

<sup>2</sup>*H. Hulubei NIPNE and IGE Foundation, Bucharest, Romania*

<sup>3</sup>*GREMI, CNRS - Universite d'Orleans, Orleans, France*

<sup>4</sup>*Scientific Center "Institute for Nuclear Research", Kiev, Ukraine*

<sup>5</sup>*Air Force Office of Scientific Research, AFOSR/NE, 801 N. Randolph, St. Arlington, VA 22203-1977, USA*

**Abstract.** Because of the high density of energy storage and the large cross section for its release, nuclear spin isomers have attracted considerable recent interest. The triggering of induced gamma emission from them has encouraged efforts to develop intense sources of short-wavelength radiation. One of the more interesting examples is the  $16^+$  4-qp isomer of  $^{178}\text{Hf}$  which stores 2.445 MeV for a half-life of 31 years meaning that as a material, such isomeric  $^{178}\text{Hf}$  would store 1.3 GJ/g. Recently, a sample containing  $6.3 \times 10^{14}$  nuclei of the isomer of  $^{178}\text{Hf}$  was irradiated with X-ray pulses derived from a device operated at 15 mA to produce bremsstrahlung radiation with end point energies set to values between 60 and 90 keV. Emission of gamma radiation from the sample was increased by 1–2% above the quiescent value of spontaneous emission. Such an accelerated decay of the  $^{178}\text{Hf}$  isomer is consistent with an integrated cross section of  $2.2 \times 10^{-22} \text{ cm}^2 \text{ keV}$  if the resonant absorption of the X-rays takes place below 20 keV as indicated by the use of selective absorbing filters in the irradiating beam. The work reported here describes the current experimental focus and results recently obtained with the use of coincident detection of emitted gamma photons by several detectors.

**Key words:** nuclear spin isomers, induced gamma emission.

### 1. Introduction

At low energies there are similarities between structures of the excited states of atoms and nuclei that encourage studies of the analog for nuclei to the phenomenon of resonance fluorescence in atoms. Both systems involve the storage of energy in the quantized movement of the constituent charges. In atoms electrons populate excited states which can be conveniently described in terms of single-particle orbitals. In nuclei the neutrons appear as relatively negative concentrations in the overall positive fluid of the nucleus; so there is the possibility to store energy by raising either protons or neutrons, or both, up distinctly separate "ladders" of excited single-particle states. Many interesting cases occur in nuclei deformed from the

idealized spherical shape and the possibility for long-lived metastability is clear [1], just as it is in the atomic analogs. However, while difficulties in arranging suitable lifetimes for populations of metastable states at the atomic level has inhibited the development of practical devices, at the nuclear level spin isomers store excitation at densities of GJ/g for decades.

In either the case of atoms or nuclei the energy stored in the population of excited states is often released by the spontaneous emission of electromagnetic radiation. Atoms emit photons of light and X-rays while nuclei emit gamma photons, but the principles and selection rules remain the same. When spin of the constituent particles is introduced into the models, the possibility for long-lived metastability results. In those cases spontaneous emission is “forbidden” for simple dipole transitions because there is no lower energy state to which the excited particle could “fall” without overturning its spin, a step particularly forbidden by selection rules. More characteristic of just the nuclear systems, is the formation of “mixed states” which have been considered as important for the triggering of the release of the metastability. Besides a mixing of charge identities that has no analogy at the atomic level, there are possibilities for mixings of other types, such as those introducing properties resulting from the quantized rotation of the aspherical nucleus as a whole, or even from oscillation between prolate and oblate asymmetries [1, 2]. By introducing additional degrees of freedom from such mixings, more transitions may become allowed that would facilitate subsequent decay. With the demonstration that induced gamma emission is possible by scattering X-rays from such materials, considerable interest had been developed in the study of these processes because it had seemed that mixed states were involved [2–5].

## 2. Theoretical model

In the terminology of nuclear physics, electromagnetic transitions between excited states of nuclei such as those described in the previous section are called  $(\gamma, \gamma')$  reactions, the first  $\gamma$ , being the absorbed photon (actually an X-ray) and the second  $\gamma'$ , being an output photon of fluorescence, often resulting from transitions in the yrast band [1]. A schematic diagram of the process is shown in Figure 1 which identifies a  $j$ -th intermediate level, or  $K$ -mixing level, or “gateway”, excited in a  $(\gamma, \gamma')$  reaction. Most intense sources of keV to MeV photons emit continua, such as bremsstrahlung. Thus the principal figure of merit for a transfer of population to a fluorescence level through the gateway state is the integrated cross section [6],  $(\sigma \Gamma) \equiv \pi b_a b_o \Gamma \sigma_0 / 2$ , whether or not the initial state being excited is the ground state or a long-lived isomeric state. The integral is taken over the lineshape of the absorption resonance within which there is little variation of the spectral intensity of irradiating continua. Constituent parameters in the integrated cross section are the peak value of the Breit–Wigner cross section [7],  $\sigma_0$  which depends on the square of the wavelength of the incident photon, the branching ratio for decay of the gateway to the fluorescence level,  $b_o$ , and the radiation width for decay of the

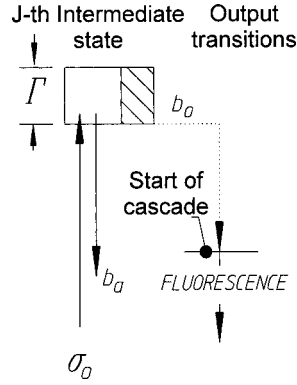


Figure 1. Schematic representation of the decay modes of a gateway state of width  $\Gamma$ . The initial state from which population is excited with an absorption cross section  $\sigma_0$  can be either ground or isomeric.

gateway back to the initial state,  $b_a\Gamma$ . The corresponding branching ratio is  $b_a$  and  $\Gamma$  is the natural width of the pump state. The maximum value of the partial width,  $b_a b_o \Gamma$  occurs when  $b_a = b_o = 0.5$ .

It is well established [5, 6, 8–10] that the population,  $N_f$  transferred or “pumped” to the final, fluorescence level is given in the case of a sample that is optically thin at the pump wavelength by

$$N_f = N_i \Phi_0 \int_0^{E_0} \sigma(E) F(E, E_0) dE, \quad (1)$$

where  $N_i$  is the initial, target population. The irradiating photon continuum is described by a total time-integrated flux  $\Phi_0$  and the function  $F(E, E_0)$  which gives the relative spectral intensity at each of the gateway energies  $E = E_j$  within the continuum whose endpoint energy is  $E_0$ . Thus  $F(E, E_0)$  is normalized such that its integral over the entire spectrum is unity. The summation allows for pumping (or triggering) to occur simultaneously through more than one gateway by resonant absorption. Only discrete pump bands are excited at energies below the threshold for particle evaporation [11] so that  $\sigma(E)$  has the form of a sum of delta functions with singularities at the gateway energies  $E = E_j$ . Integrated cross sections are determined from Equation (1) using measured yields of fluorescence-state production and known irradiating spectra.

### 3. Experimental model confirmation

In experimental work of the mid-80’s to mid-90’s, bremsstrahlung from six accelerators in different experimental environments was used to verify the fluorescence model of Equation (1) and to cross-check the accelerator intensities [3, 9, 12]. The devices involved in those efforts were DNA/PITHON at Physics International, DNA/Aurora at the Harry Diamond Laboratories, 4-MeV and 6-MeV medical

linacs at the University of Texas Health Sciences Center, the superconducting injector to the storage ring at Darmstadt (S-DALINAC), and the TEXAS-X 4-MeV research linac at the University of Texas at Dallas. The established EGS4 coupled electron/photon transport code [13] was adapted for each individual irradiation configuration to determine both  $F(E, E_0)$  and  $\Phi_0$  from closely monitored values of accelerator currents. In some cases  $\Phi_0$  was separately verified by in-line dosimetry [9].

In these experiments gram-sized samples were irradiated for times ranging from seconds to hours for the continuous wave (cw) machines and by single flashes from the pulsed devices. The experimental results [4, 5, 8, 14–16] were in close agreement with the predictions of Equation (1) used with literature values [17] of  $(\sigma\Gamma)_{ff}$ . The most detailed confirmation of theory was obtained with the reaction  $^{87}\text{Sr}(\gamma, \gamma')^{87}\text{Sr}^m$  which was used for calibration purposes [3, 5, 9]. Particularly valuable were the data obtained with the S-DALINAC whose bremsstrahlung endpoint could be continuously varied to change  $\Phi_0$  and modulate the intensity function  $F(E_j, E_0)$  at the critical energies,  $E_j$ . The largest effect was found to occur when  $E_0$  was swept from just below a gateway at  $E_j$  to just exceeding it. This produced sharp “activation edges” which identified gateway locations in excitation functions obtained by plotting the final-state yield against endpoint.

Figure 2 displays an excitation function measured [3, 5, 9] for the calibration reaction  $^{87}\text{Sr}(\gamma, \gamma')^{87}\text{Sr}^m$  obtained with four of the accelerators, along with a curve calculated from literature values [5, 17] for the parameters of the intermediate “gateway” transitions. The fifth of the available accelerators operated at the higher energies for which there were no available literature values for calibration, so those

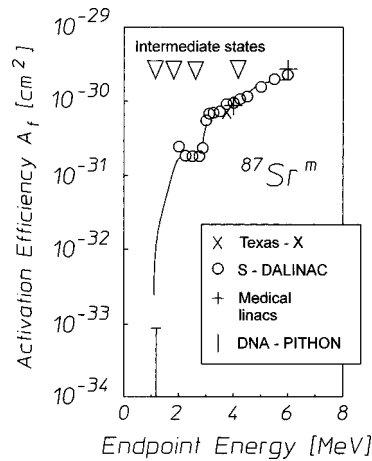


Figure 2. Actual excitation function [3, 5] for the reaction  $^{87}\text{Sr}(\gamma, \gamma')^{87}\text{Sr}^m$  plotting  $A_f$  as a function of bremsstrahlung endpoint. The solid curve shows values computed from Equation (1) using gateway parameters from the literature [5, 17] (indicated by arrows) and calculated photon spectra.

results are not shown in Figure 2. At the lowest energy only the upper limit for a null result can be shown on this logarithmic scale. The yield is expressed as an “activation efficiency”,  $A_f \equiv N_f/(N_i\Phi_0)$  in units which are correspondingly small in magnitude since the fractional yield is normalized to the total flux in the continuum, most of which is not located at the gateway energies. As can be seen in the figure, there is excellent agreement between measurements obtained with accelerators emplaced in entirely different environments, and between the experimental data and the model calculations. Calibration studies like this example both confirmed the traditional model of “optical pumping” in  $(\gamma, \gamma')$  reactions of Equation (1) and validated the use of the EGS4 code for calculating bremsstrahlung intensities from measured accelerator parameters.

#### 4. Giant $(\gamma, \gamma')$ resonances

For nuclei deformed from the spherical shape the quantum number of dominant importance that insures metastability is  $K$ , the projection of individual nucleonic angular momenta upon the axis of elongation [1, 18]. In order to release the energy stored in a spin isomer an electromagnetic transition that started from it must span a substantial change in  $K$  and component transitions, such as shown in Figure 1, had been expected to have large, and hence unlikely, multipolarities.

From this perspective, the isomer  $^{180}\text{Ta}^m$  was one of the most initially unattractive of any of the isomers as it required a change of both  $\Delta J = 8$  of angular momentum and  $\Delta K = 8$  for the projection between isomer and ground state. However, because a macroscopic sample was readily available in mg quantity,  $^{180}\text{Ta}^m$  became the first isomeric material to be optically pumped to a fluorescent level. The  $^{180}\text{Ta}$  nuclide is the rarest stable isotope found in nature at 0.012% abundance and is the only naturally occurring isomer. The  $1^+$  ground state has a half life of 8.1 hours while the  $9^-$  isomer,  $^{180}\text{Ta}^m$  stores 75.3 keV with a half life in excess of  $1.2 \times 10^{15}$  years [17].

In an experiment conducted in 1987, 1.2 mg of  $^{180}\text{Ta}^m$  was exposed to bremsstrahlung from the 6 MeV linac at the University of Texas Health Sciences Center and a large fluorescence yield was obtained [4]. This was the first time a  $(\gamma, \gamma')$  reaction had been excited from an isomeric target and was the first evidence of the existence of “giant pumping resonances” as transitions to  $K$ -mixing levels were called at those times. Simply the observation of fluorescence from a milligram-sized target proved that an unexpected reaction channel had opened since grams of material had been usually required in this type of experiment. Analyses [4, 19] of the data indicated that the partial width for the dumping of  $^{180}\text{Ta}^m$  was nearly 0.5 eV.

Gateway transition energies were determined for the  $^{180}\text{Ta}^m(\gamma, \gamma')^{180}\text{Ta}$  reaction in a series of irradiations [5] made at the S-DALINAC facility using fourteen different endpoints in the range from 2.0 to 6.0 MeV. Twelve of the irradiations at the higher endpoint energies produced measurable levels of fluorescence. Figure 3

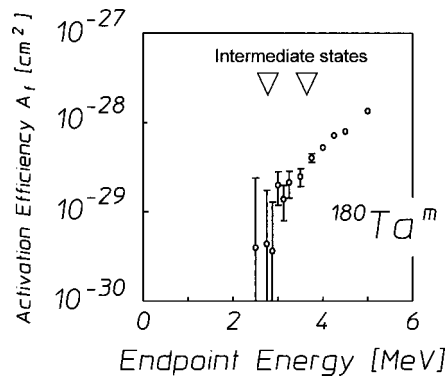


Figure 3. Excitation function [5] for the reaction  $^{180}\text{Ta}^m(\gamma, \gamma')^{180}\text{Ta}$  plotting  $A_f$  as a function of bremsstrahlung endpoint. Fitted gateway locations are indicated by the arrows.

displays the resulting excitation function showing a clear activation edge. Fitting of the data to Equation (1) by adjusting trial values of  $(\sigma\Gamma)_{fj}$  determined integrated cross sections for the dumping of  $^{180}\text{Ta}^m$  isomeric populations into freely-radiating states. Values [5] were  $12,000 \times 10^{-29} \text{ cm}^2 \text{ keV}$  and  $35,000 \times 10^{-29} \text{ cm}^2 \text{ keV}$  for gateways at  $2.8 \pm 0.1 \text{ MeV}$  and  $3.6 \pm 0.1 \text{ MeV}$ , respectively.

The integrated cross sections for  $^{180}\text{Ta}$  were surprisingly large, being 10,000 times greater than the values usually measured for nuclei [6, 8, 14–16]. However, a question could be raised about whether they describe transitions through single intermediate gateway states. The data of Figure 3 is not so clear as in the calibration of Figure 2 and conceivably could be described by a threshold process in which all photons with energy above threshold participate, as in particle reactions. The form of the excitation function is different in the two cases, but not so much as to support an unequivocal identification of which form is followed by the data of Figure 3. However, at these energies of a few MeV the initial photon is absorbed without the possibility of evaporating a particle from the nucleus and it is not clear what other process could lead to continuous absorption above some threshold. Resonant absorption to closely spaced states where the state density was high would be another more likely possibility. In that case what was reported as a transition to a single state might have been distributed among many states occupying the band of energies within which resolution of the experiment could not separate individual components.

A survey of 19 isotopes [9] conducted with four of the U.S. accelerators over a fairly coarse mesh of bremsstrahlung endpoints confirmed the existence of other gateway transitions with such large integrated cross sections as to be termed “giant pumping resonances” in the island of masses near 180. Measured excitation functions continued to identify integrated cross sections for pumping and dumping of isomers that were on the order of 10,000 times greater than usual values. Higher-resolution studies [20] with the S-DALINAC showed that the giant pumping resonances reappeared at lower masses near 120. It was demonstrated [9, 21]

that both the magnitude of pumping strength and the gateway excitation energies varied slowly among neighboring isotopes within each mass island seen in Figure 4.

The key to successfully using X-rays to transfer population from a long-lived isomer to a short-lived fluorescence level lies in the existence of these giant pumping resonances, now supposed to be electromagnetic transitions to  $K$ -mixing levels. Gateways of this strength represented an unusual nuclear structure that provides for the spanning of large  $\Delta K$  between ground state and isomer. The mediating states may be " $K$ -mixing levels" described by superposition of eigenfunctions corresponding to several different projection quanta,  $K$  but to comparable values of  $J$  not too different from that of the isomer and from the band built on the ground state. Low multipolarity transitions to and from the  $K$ -mixing gateway could provide the type of giant pumping resonance indicated by the measurements.

The first evidence [4, 5] for the existence of giant pumping resonances had been the dumping of  $^{180}\text{Ta}^m$  to its ground state through  $\Delta K = -8$ . In that instance, an X-ray photon had to be absorbed by a gateway lying at  $2.8 \pm 0.1$  MeV above the isomer so spontaneous decay of the isomer through the  $K$ -mixing level could not have occurred without the pumping. This gave the isomer its exceedingly long lifetime. However, in 1990 the 4-qp isomer  $^{174}\text{Hf}^m$  was observed [22] to decay by proceeding through a state of mixed  $K$  lying at 2.685 MeV and providing  $\Delta K = -14$  to reach the ground-state band. Since this  $K$ -mixing level lay lower in energy than the isomer, spontaneous decay was possible and the lifetime of the initial metastable state was only  $3.7 \mu\text{s}$ . The similarity of the excitation energies of the  $K$ -mixing gateways for  $^{180}\text{Ta}^m$  and  $^{174}\text{Hf}^m$ , as well as those for other giant pumping resonances summarized in Figure 4 led to a further examination of the systematics. In most cases the excitation or deexcitation of the initial state always occurred in the direction tending to reduce the value of  $K$ , in agreement with per-

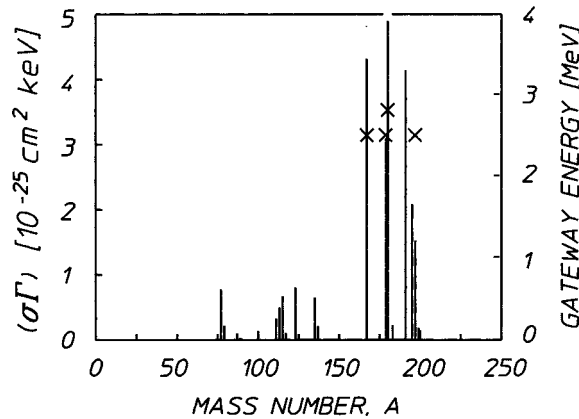


Figure 4. Bars and X's, respectively, plot integrated cross sections and gateway energies for pumping isomers from the surveys of [3, 5, 9, 21] on left and right axes, respectively. The groupings correspond to mass islands between magic numbers for the nucleons.

ceptions that reactions generally proceed toward the yrast. While the details were not known, there could be global appreciation that the first absorption occurred with a small  $\Delta K$  to reach a gateway state not too unlike the initial state in single particle structure and then subsequent cascade proceeded toward the yrast levels as expected.

Somewhat overlooked for years were the contradictory results for 3 reactions, those ( $\gamma$ ,  $\gamma'$ ) reactions exciting isomers from the ground states of  $^{176}\text{Hf}$ ,  $^{191}\text{Ir}$ , and  $^{195}\text{Pt}$ . Those were excited through the “giant pumping resonances” even though there were changes of  $\Delta K = +6$ ,  $+4$ , and  $+5$ , respectively [3, 9]. Most challenging must be the excitation of the first because it is (even, even) and it is difficult to understand the origin of such an increase in angular momentum and its projection that must arise from the initial absorption of a single photon. If these effects belong to narrow absorption resonances and still result in such unlikely increases in angular momenta, then further investigation of the structure of possible collective excitations between 2 and 3 MeV deserves attention.

The most interesting of the nuclear metastables may be the  $16^+$  4-qp isomer of  $^{178}\text{Hf}$  in which one member of a pair of both protons and neutrons is raised in energy to the next open excited state and “flipped” in spin so that spontaneous emission of electromagnetic radiation is doubly “forbidden” by selection rules applying both to the protons and to the neutrons [1]. These states store 2.445 MeV for a half-life of 31 years meaning that as a material, such isomeric  $^{178}\text{Hf}$  would store 1.3 GJ/g. Small samples exist for experimentation and the stored energy has been released by exciting the isomeric state to a higher level of mixed composition from which spontaneous decay was no longer forbidden [23–25]. The details of this remarkable result have been recently and thoroughly described [23–25] and so will be reviewed here only briefly. The trigger excitation was provided by the resonant absorption in the nucleus of a photon of less than 20 keV energy and the energy gain per event exceeded 100-fold. The source of X-rays was a small device normally used in dental medicine. It used pulsed currents in an X-ray diode to produce an uncollimated beam of bremsstrahlung with end point energies that could be selected between 60 and 90 keV. In general use the peak flux was of the order of  $5 \times 10^{10}$  photons  $\text{cm}^{-2} \text{sec}^{-1} \text{keV}^{-1}$ . A graphic result showing the increases in the numbers of fluorescent gamma photons when the target was illuminated is shown in Figure 5. Seen there are enhancements of the order of 1–2% induced by the irradiation above the steady rate of spontaneous emission from the decay of the  $^{178}\text{Hf}$  isomer. The leftmost line of the doublet to the left of the figure, together with the lines in the middle and right of the figure, comprise the 2nd, 3rd, and 4th members of the Ground State Band (GSB,) that usually dominates the spontaneous emission from the isomer. In Figure 5 the data were not specifically corrected for the variations of detector efficiency with energy because only fractional increases in spontaneous emission were used in actual analyses. However, the variation with energy of the absorption introduced by layered shielding used to selectively remove X-rays scattered from the irradiation source tended to compensate the decrease in

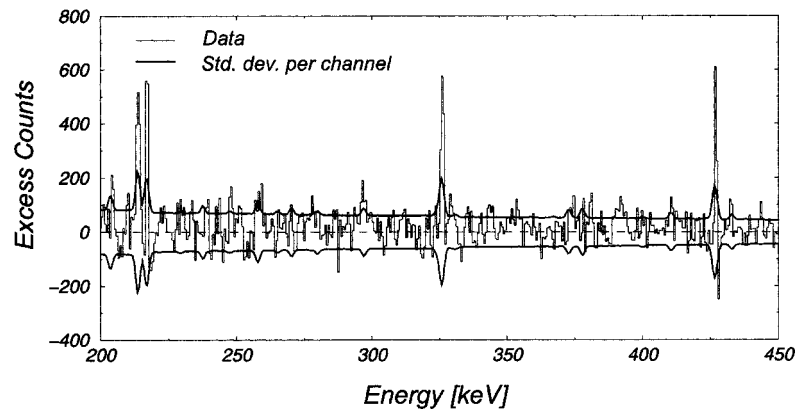


Figure 5. Difference in counts obtained in the spectra of  $^{178}\text{Hf}$  with and without irradiation by X-rays. Curves showing values computed for  $1\sigma$  for each channel of energy by the usual methods for propagating errors are shown.

efficiency of the detector at higher energies; so that representations such as Figure 5 remain useful to illustrate the visibility of the effect.

The specific numbers of counts in quiescent and induced emissions from the  $^{178}\text{Hf}$  isomer were reported in detail and were used in quantitative analyses of the measurements [25]. The overall confidence factor for the composite observation of the three lines shown is greater than  $6\sigma$ , meaning less than one chance in  $10^8$  that the enhancement is simply accidental. From the numerical values associated with the data of Figure 5, the corresponding rates measured for spontaneous emission, and the measured flux of incident X-rays, the integrated cross section was obtained from Equation (1) to be  $2.2 \times 10^{-22} \text{ cm}^2 \text{ keV}$ , if it is assumed that the resonant gateway transition was excited by the component at 20 keV. A value of 20 keV greater than the 2445 keV stored by the  $^{178}\text{Hf}$  isomer would suggest that a  $K$ -mixing level at 2.465 MeV was responsible, in good agreement with the general trend for a slow variation of the energy of the “gateway” or  $K$ -mixing levels noted above and shown on Figure 4. However, the value of the integrated cross section is even more elevated than the magnitudes of  $10^4$  found in the previous survey above what is expected for “ordinary” ( $\gamma, \gamma'$ ) reactions. This value reported for  $^{178}\text{Hf}$  is  $2.2 \times 10^7$  greater than the usual  $10^{-29} \text{ cm}^2 \text{ keV}$ . Such elevation is consistent with the increase in the Breit–Wigner cross section with decreasing transition energy, *if the widths of the transitions appearing in Equation (1) remained roughly constant.*

Neither the quantum structure of the mixed state excited by the incident X-rays nor the precise energy of excitation has been determined in the case of  $^{178}\text{Hf}$ . Nevertheless, because of the high density of energy storage and the large cross section for its release there is considerable significance of this triggering of induced gamma emission from nuclear spin isomers to efforts to develop intense sources of short-wavelength radiation. The work reported here describes the current experimental focus and results most recently obtained.

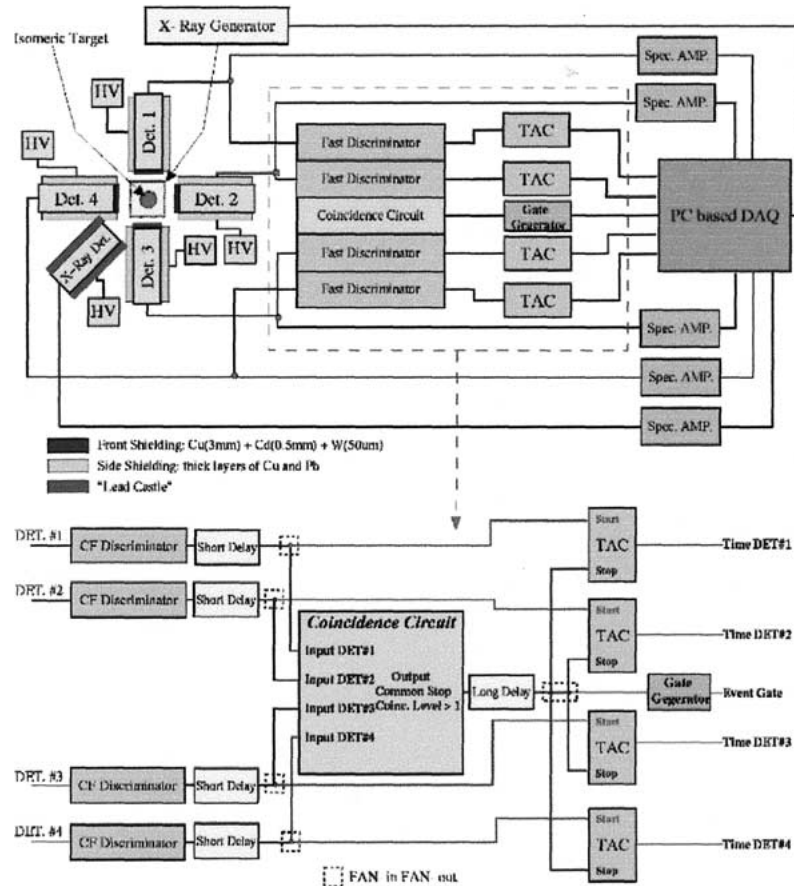


Figure 6. Schematic drawing of the apparatus.

## 5. Experimental arrangements

Progress in 2000 in the Texas Group with its international affiliates benefited from a complete redesign and implementation of the experimental system as shown in Figure 6. Four 10% Ge detectors were installed to support coincidence measurements of the  $\gamma$  photons from decay of the  $^{178}\text{Hf}$  isomers triggered by the X-ray irradiation. Continuous A/D conversion of the signal from the spectroscopy amplifiers with virtual instrument technology eliminated “deadtime” of data acquisition. Synthesized voltages to the X-ray head stabilized irradiation of the isomeric targets. A 5th detector recorded the spectrum of the X-ray irradiation by observing what was scattered from the isomeric target. Energies and times of detection of individual photons were recorded for each of the detectors. Operating currents and X-ray fluxes were continuously logged.

The same X-ray head commercially available for use in dental examinations was driven with a synthesized waveform to produce bursts of 100 rectangular cur-

rent pulses as shown in Figure 7. Data were logged during a full burst and then processed during the quiescent period between bursts. Heating of the filament in the X-ray tube changed its impedance during the first 10 pulses of a burst, but after that currents and voltages remained stable for the last 90 pulses in a burst. Seen in the inset is typical data for the last 90 pulses and shows that there is a period of stability for current and voltage persisting for 1 ms duration in the middle part of each of the last 90 pulses in a burst.

As a result of these modifications of the X-ray source, greater stability of the spectrum of the irradiation was achieved. Figure 8 shows the evolution of the spectrum of the X-ray flux during a typical burst of irradiation. Direct measurement showed a noticeable alteration during the first 10 pulses in a burst of irradiation characterized by a substantial reduction of the end point energy of the bremsstrahlung component of the X-rays. However, high stability can be seen in the end point energies during the last 90 pulses in each burst. In the inset the end point energies are seen to vary only from 61 to 60 keV. The strong variation during the first 10 pulses offers additional opportunity to “sweep” the bremsstrahlung energies of the irradiating spectrum to search for any sharp onset of further increases in the triggering of the decay of the isomers that could be associated with transitions to higher energy trigger levels.

Study of the direct coupling of electromagnetic interference (emi) from the power supply to the X-ray source into the data acquisition system guided in the optimization of shielding against the emi. Figure 9 shows the resulting noise levels. What is shown is the counting rate of  $\gamma$  photons from the spontaneous decay emitted by the isomeric target as a function of the time from the start of irradiation

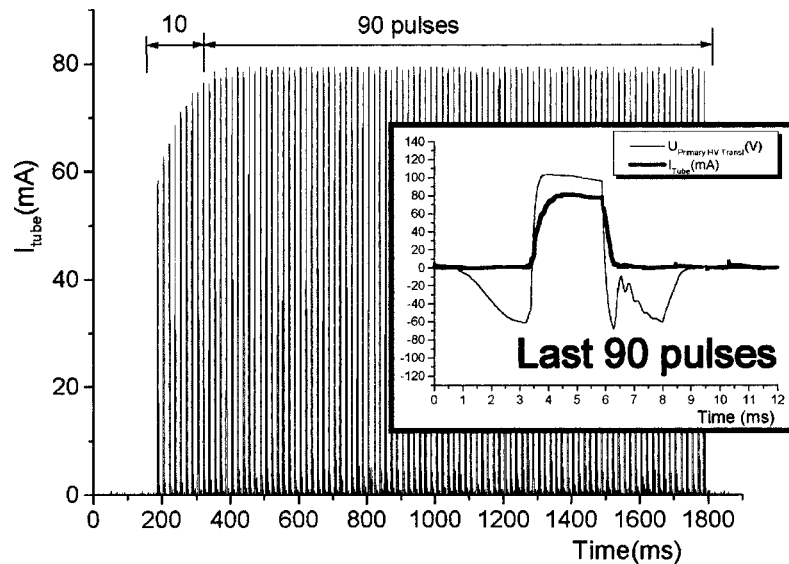


Figure 7. Currents and voltages supplied to X-ray source.

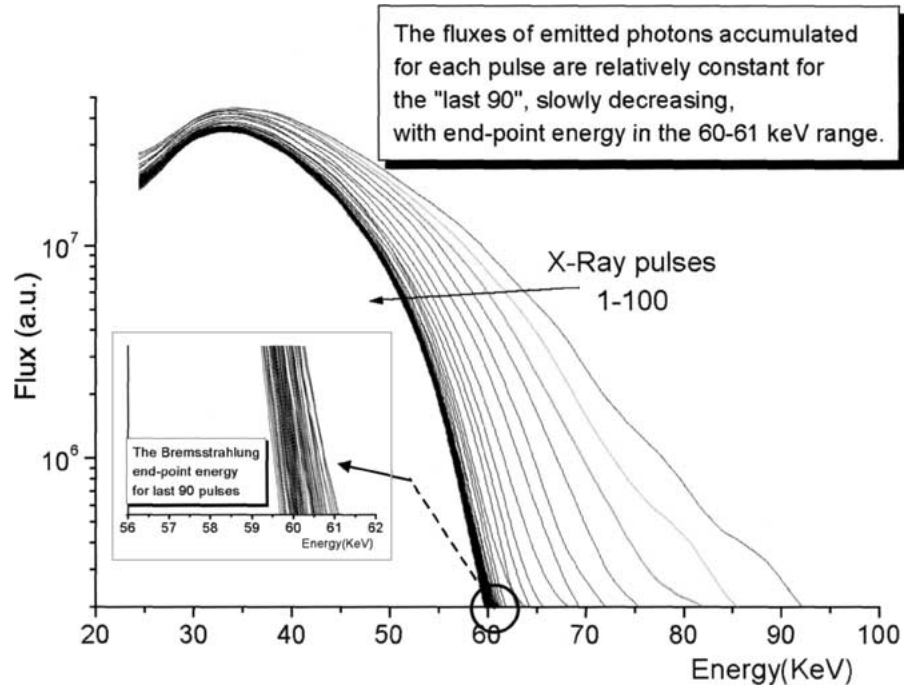


Figure 8. Performance of the X-ray source built in 2000.

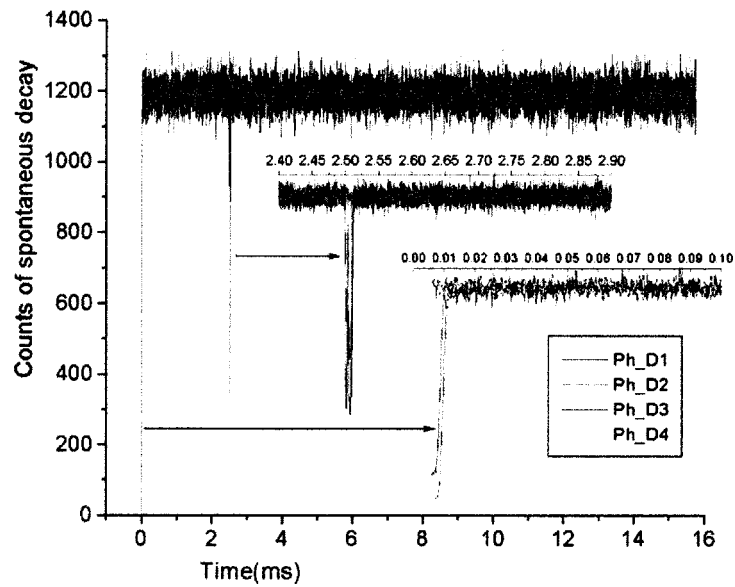


Figure 9. Measurement of  $\gamma$  emission from the spontaneous decay in the isomeric target recorded with each Ge detector.

during a single pulse in a burst. What can be seen is that the effect of residual emi was to suppress the counting rate of the spontaneous emission in some detectors by overloading the acquisition system. However, with the higher resolution shown in the insets those periods of interference were sharply limited to  $30 \mu\text{s}$  intervals at the beginning and end of the current pulses to the X-ray head. In practice data is simply not recorded during those intervals and the effects of emi are thus avoided.

## 6. Recent results

Figure 10 presents a simple overview of the challenges and strengths of the use of coincidence techniques to enhance data analysis. Pairs of photons detected by any 2 of the 4 detectors define a coincidence event. If they arrive within a selected period, currently set to be 10 ns, the energies of each photon of the pair are used as the  $(x, y)$  coordinates at which a “count” is recorded on a 2-dimensional map such as shown on the figure. As counts build totals at some of the map coordinates, the greater totals are indicated by greater density. A sample map is shown in Figure 10. Low photon energies start in the lower left. In the horizontal direction the scale is such that the full range 0–1000 keV is covered. In the vertical direction the scale has been stretched so that only the approximately 40 keV around the important Hf-lines and impurity calibration lines are shown in detail. In analogy with astronomy, in the photo some structures can be seen that are localized in particular rows and columns that tell the energies of each of the photons collected at the same time to within 10 ns. The merit of a good coincidence system such as seen here is that there should never be a “line” with row and column belonging to different nuclides. The principal difficulty is that such a coincidence spectrum has 4 million pixels to

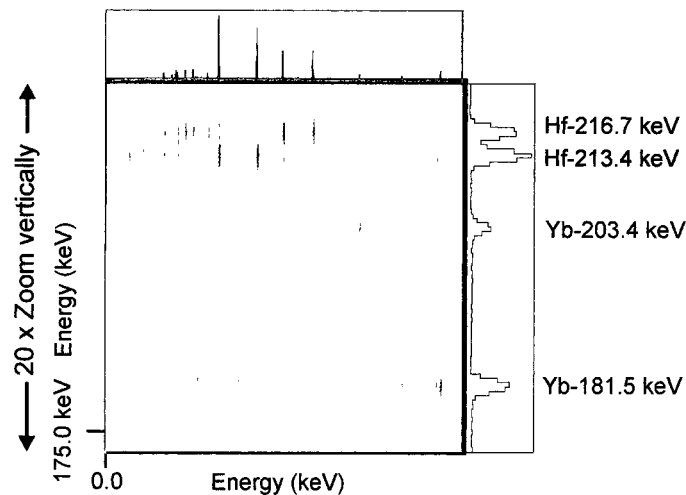


Figure 10. Map of the energies of two photons detected within the same 10 ns interval in two different detectors.

examine for “new” lines that might show in the data collected during irradiation that are not found in the spontaneous decay of the isomeric nuclei.

Once a region of interest is identified, the data can be analyzed by selecting a narrow “row” of interest in a display such as shown in Figure 10. Figure 11 shows such an example. In the upper right panel is shown the spectrum “sliced” out of the matrix along a row defined by the darkened line seen in the upper left panel. A “new” line at 129.5 keV found only during X-ray irradiation defines a coincident “row” in which is found only the 213.4 keV member of the ground state band (GSB) of the  $^{178}\text{Hf}$  nuclide. For comparison, the lower two panels show the same comparisons for the “row” gated by the 88.8 keV (8–, 8+) band that feeds the entire GSB by subsequent cascading of transitions from the top, down, all occurring in less than 10 ns. The lower right panel enlarged from that “row” shows the entire GSB as expected. From this preliminary data, it is indicated that a new line in the decay spectrum of the  $^{178}\text{Hf}$  isomer at 129.5 keV is excited only during the decay triggered by the X-ray irradiation and it cascades into the lower part of the GSB that subsequently cascades further only into the 213.4 keV transition. Confidence in this type of analysis is enhanced by the choice for comparison with the 129.5 keV line of a line such as 88.8 keV that is proximate in energy and comparable in detected counting rate.

Data such as shown in Figure 11 were not corrected for detector efficiency as they were used only to locate component lines of “new” decay cascades induced by the X-ray irradiation. At these lower energies the absolute intensities were strongly affected by three factors: the front shielding that had been designed to cut off energies below 90 keV, the slowed timing response of large Ge detectors to

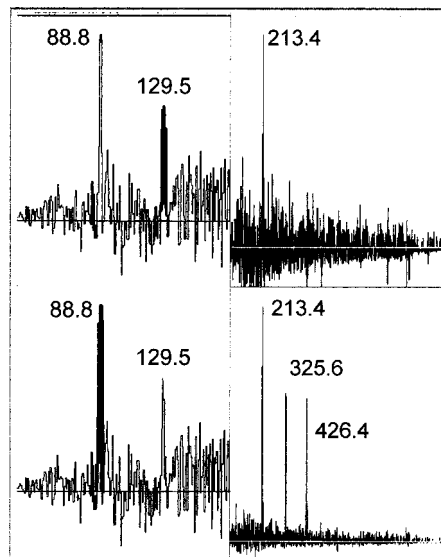


Figure 11. Example of “new” line found in coincidence data.

lower energy photons, and the settings of constant fraction thresholds. The combined effect was sharply lowered sensitivity with decreasing photon energy below 100 keV. The intensity of the 88.8 keV line was actually much greater than that of the 129.5 keV line, but the counting rates actually detected are similar as seen in Figure 11.

In reducing data to the level shown in Figure 11 two levels of background had to be removed. The first was a subtraction from the entire map used to produce Figure 10 of the array of accidental coincidences. As the term implies, such events were the result of two detectors accidentally collecting photons within 10 ns of each other that did not arise from a single decay cascade. These were removed by subtracting the projections onto the axes of the spectra; and were not varied over the course of the analyses. The second concerned the removal of the Compton continuum that represented “true” coincidences between events which occurred as part of a single decay cascade. However, only one of the detectors collected a photon directly from the decay while the other collected a photon reduced in energy by a Compton event along the way. These were removed from a spectrum of a row gated by a line such as those shown as darkened in one of the left-side panels of Figure 11 by subtracting a second scaled spectrum obtained by gating on the rows corresponding to the regions immediately to the left and right of the line. Such a process is most reliable when the lines used for gating are proximate in energies and comparable in intensities.

The preliminary data available for presentation in this work represented the continuous collection of data for only 30 calendar days of operation. Nevertheless, it satisfied the validation tests as discussed above and then served to support identification of a new line characteristic of the triggering of the decay of the  $^{178}\text{Hf}$  isomer. While the technique appears proven, substantially longer periods of data acquisition will be necessary to support more comprehensive evaluation of the pathways through which the triggered decay proceeds toward the ground state.

The identification of the new line at 129.5 keV excited in coincidence with the 213.4 keV member of the GSB is further supported by histograms for the detection of those particular coincidences. In the course of the direct digitization of the spectroscopy amplifiers, the arrival times of each photon at each detector is logged to a precision of 250 ps for the evaluation of possible coincidences. Thus it is possible to separate out the time and energy records for the  $100 \pm 20$  pairs of photons contributing the apparent peak in the plots such as Figure 11. Shown in Figure 12 is the distribution between the 6 possible pairs of the 4 Ge detectors of the coincident events in which a photon at 129.5 keV was detected at a time within 10 ns of that at which a 213.4 keV photon was detected in another detector. The distribution is uniform to within statistical errors as must be the case if those coincidence events are not artifacts from a few of the detectors. Shown in Figure 13 is the histogram for the distribution of the coincident events involving both a 129.5 and a 213.4 keV photon among the possible “phase times” between the start of one

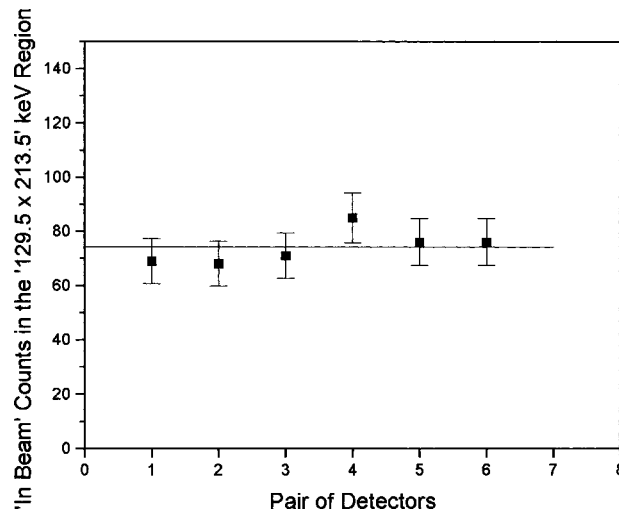


Figure 12. Distribution of the origins among the 6 possible pairings of the 4 detectors of each of the pairs of photons detected at two different detectors within the same 10 ns interval when one photon had energy 129.5 keV and the other 213.4 keV.

pulse of irradiation and the start of the next one. Here the excess of counts collected during the period of irradiation is striking. Passing such tests based upon these histograms is a necessary condition to establish the 129.5 keV emission as a new transition induced by the irradiation, but only additional data can prove sufficient to verify this interesting indication.

After completion of this manuscript just such further confirmation of the excitation of this new line from the induced decay of the isomer was obtained. The synchrotron radiation source, SPring-8 was used to irradiate a sample of  $^{178}\text{Hf}$  isomers at considerably greater intensity. Figure 14 shows the clear appearance of the “new” line in single-photon spectra [26]. The enhancement is sufficient to determine the transition energy to be 129.4 keV in agreement with the results reported in this work.

## 7. Conclusions

Figure 15 shows a small part of the energy level diagram for the  $^{178}\text{Hf}$  nucleus. Only the relatively few levels through which transitions pass during the spontaneous decay of the isomer have been shown. Since the nucleus has prolate deformation the scheme superficially resembles that for a diatomic molecule with “rotational bands” being built upon intrinsic states of single-particle excitation. Besides the 4-qp isomer,  $16^+$  only the two intrinsic states used above as examples are important in the spontaneous decay of the  $^{178}\text{Hf}$  isomers. Transitions between members of the rotational bands built upon those two contribute most of the lines seen in the spectrum of spontaneous emission. The two bands are the ground state band, GSB

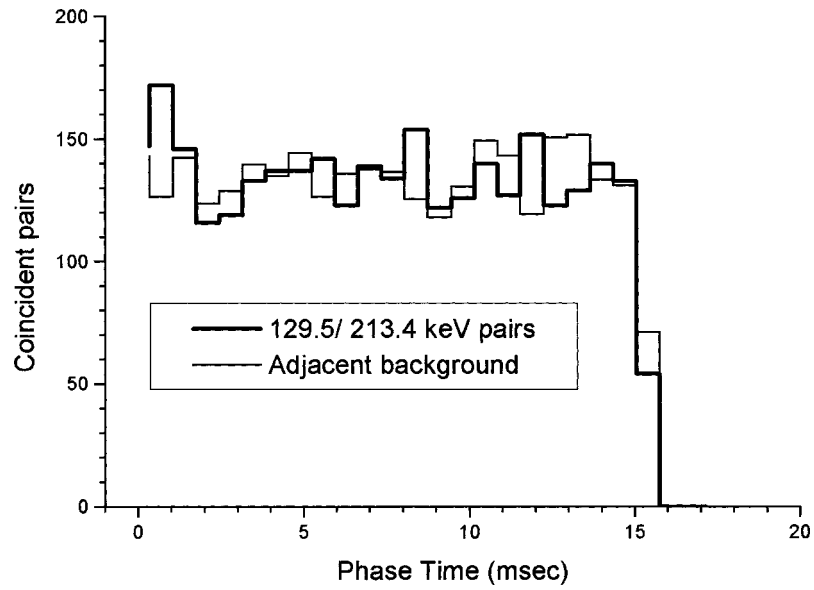


Figure 13. Distribution of photon pairs from Figure 12 among the possible time intervals for detection between the start of one pulse of irradiation of the target and the start of the next irradiation.

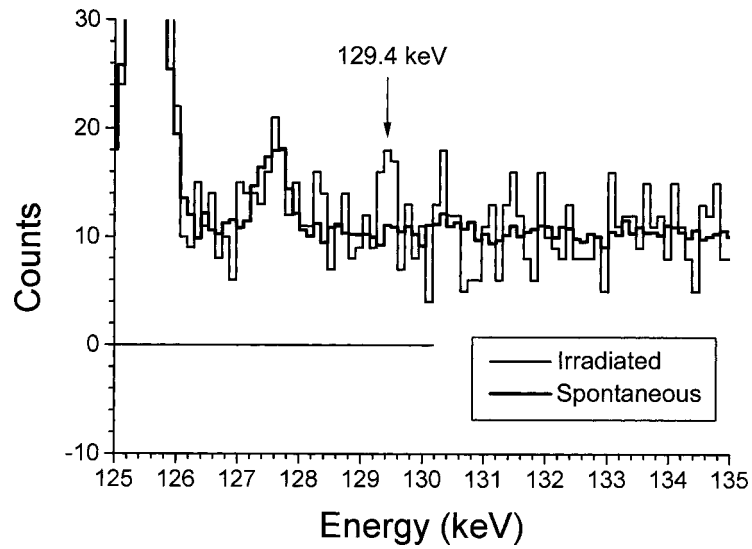


Figure 14. Data confirming the excitation of a new transition during decay induced by synchrotron radiation at higher intensities. For comparison the spectrum of spontaneous emission from the target is shown. Improved intensity shows the transition energy to be 129.4 keV.

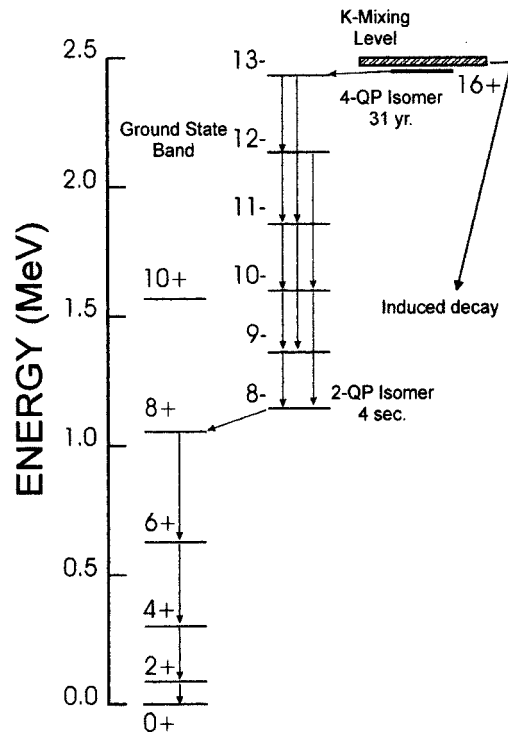


Figure 15. Schematic diagram of the nuclear energy levels important in the spontaneous decay of the spin isomer  $^{178}\text{Hf}$ .

and the  $8^-$  band and they are connected by the interband transition at 88.86 keV which is delayed by the 4 sec half-lifetime of the  $8^-$  bandhead. However, in the actual target used in these experiments, lines from daughter nuclei from the decay of  $^{172}\text{Hf}$  impurities complicate the data collection. Only about 5.7% of the events logged arise from transitions in the GSB of  $^{178}\text{Hf}$  and those contribute the most prominent parts of the spectrum.

The work reported here continues to confirm that the irradiation of samples of 4-qp isomers such as  $^{178}\text{Hf}$  with X-rays at power levels of  $\text{mW}/\text{cm}^2$  containing component lines and continua with end points greater than 20 keV [25] can materially increase the rate of decay of long-lived nuclear populations. In the particular case of  $^{178}\text{Hf}$  the half life for the storage of energy is 31 yr and the energy gain per triggering event exceeds 100-fold, making this a very interesting system. From Figure 15 it can be appreciated that the released energy most readily detected is the result of transitions between members of the GSB excited in the course of the normal spontaneous decay. However, the distribution of intensities differs. In the spontaneous decay the  $8^+$  level of the GSB is populated by the interband transition and the subsequent transitions occur in steps passing through each lower level in sequence. As a result all members of the GSB have about the same intensity in spectra of spontaneous emission. In contrast, the induced emission can be seen in

Figure 5 to be stronger in lines from transitions connecting lower members of the GSB. The X-rays excite the isomer to the mixing level from which electromagnetic transitions are no longer forbidden, but then by some path not yet identified, cascades of transitions convey the excited state population into lower members of the GSB without dropping them down in energy through the higher members. It has been indicated [25] that some newly observed lines have arisen from transitions through these induced cascades, but intensities in any one of the lines has been insufficient to fully explain the scheme of induced decay. It has been proposed that once induced, the decay from the mixing level proceeds through many parallel cascades, no one of them concentrating enough emission into a single spectral line for unequivocal detection. The preliminary coincidence data reported here appears to support this expectation by exposing the “new” transition at 129.4 keV. Current research objectives focus upon the collection of more data from which the additional decay cascades may be deduced.

### Acknowledgements

The authors gratefully acknowledge the USAF Air Force Office of Scientific Research through AFOSR Contract No. F49620-99-1-0082 for support of these experiments.

### References

1. Walker, P. M., *Hyp. Interact.* (this issue).
2. Collins, C. B., In: I. I. Popescu and C. A. Ur (eds.), *Proceedings of the First International Induced Gamma Emission Workshop IGE '97*, IGE Foundation, Bucharest, Romania, 1999, pp. 1–17. Further exploration of these nuclear analogies is available at the URL: <http://www.utdallas.edu/research/quantum/isomer/>.
3. Collins, C. B. and Carroll, J. J., *Hyp. Interact.* **107**(3) (1997) and references therein.
4. Collins, C. B., Eberhard, C. D., Glesener, J. W. and Anderson, J. A., *Phys. Rev. C* **37** (1988), 2267.
5. Collins, C. B., Carroll, J. J., Sinor, T. W., Byrd, M. J., Richmond, D. G., Taylor, K. N., Huber, M., Huxel, N., von Neumann-Cosel, P., Richter, A., Spieler, C. and Ziegler, W., *Phys. Rev. C* **42** (1990), 1813.
6. Metzger, F. R., In: O. Frisch (ed.), *Prog. Nucl. Phys.*, Vol. 7, Pergamon, New York, 1959.
7. Blatt, J. M. and Weisskopf, V. F., *Theoretical Nuclear Physics*, Dover, New York, 1979, Chapter VIII, Section 7.
8. Collins, C. D., Anderson, J. A., Paiss, Y., Eberhard, C. D., Peterson, R. J. and Hodge, W. L., *Phys. Rev. C* **38** (1988), 1852.
9. Carroll, J. J., Byrd, M. J., Richmond, D. G., Sinor, T. W., Taylor, K. N., Hodge, W. L., Paiss, Y., Eberhard, C. D., Anderson, J. A., Collins, C. B., Scarbrough, E. C., Antich, P. P., Agee, F. J., Davis, D., Huttlin, G. A., Kerris, K. G., Litz, M. S. and Whittacker, D. A., *Phys. Rev. C* **43** (1991), 1238.
10. Booth, E. C. and Brownson, J., *Nucl. Phys. A* **98** (1967), 529.
11. There are many examples, including Refs. [5–9]. See also von Neumann-Cosel, P., Richter, A., Carroll, J. J. and Collins, C. B., *Phys. Rev. C* **44** (1991), 554.

12. Carroll, J. J., Richmond, D. G., Sinor, T. W., Taylor, K. N., Hong, C., Standifird, J. D. and Collins, C. B., *Rev. Sci. Instrum.* **64** (1993), 2298.
13. Nelson, W. R., Hirayama, H. and Rogers, D. W. O., The EGS4 Code System, Stanford Linear Accelerator Center Report No. SLAC 265, Stanford Linear Accelerator Center, Stanford, CA, 1985.
14. Anderson, J. A. and Collins, C. B., *Rev. Sci. Instrum.* **58** (1987), 2157.
15. Anderson, J. A., Byrd, M. J. and Collins, C. B., *Phys. Rev. C* **38** (1988), 2833.
16. Anderson, J. A. and Collins, C. B., *Rev. Sci. Instrum.* **59** (1988), 414.
17. National Nuclear Data Center Online Evaluated Nuclear Structure Data File (ENSDF), Brookhaven National Laboratory, 1994.
18. A full discussion can be found in A. deShalit and H. Feshbach, *Theoretical Nuclear Physics, Vol. 1: Nuclear Structure*, Wiley, New York, 1990, Chapter VI.
19. Carroll, J. J., Anderson, J. A., Glesener, J. W., Eberhard, C. D. and Collins, C. B., *Astrophys. J.* **344** (1989), 454.
20. Carroll, J. J., Sinor, T. W., Richmond, D. G., Taylor, K. N., Collins, C. B., Huber, M., Huxel, N., von Neumann-Cosel, P., Richter, A., Spieler, C. and Ziegler, W., *Phys. Rev. C* **43** (1991), 879.
21. Collins, C. B., Carroll, J. J., Taylor, K. N., Richmond, D. G., Sinor, T. W., Huber, M., von Neumann-Cosel, P., Richter, A. and Ziegler, W., *Phys. Rev. C* **46** (1992), 952.
22. Walker, P. M., Sletten, G., Gjørup, N. L., Bentley, M. A., Borggreen, J., Fabricius, B., Holm, A., Howe, D., Pedersen, J., Roberts, J. W. and Sharpey-Schafer, J. F., *Phys. Rev. Lett.* **65** (1990), 416.
23. Collins, C. B., Davanloo, F., Dussart, R., Iosif, M. C., Hicks, J. M., Karamian, S. A., Ur, C. A., Kirischuk, V. I., Carroll, J. J., Roberts, H. E., Mc Daniel, P. and Crist, C. E., *Laser Phys.* **9** (1999), 8.
24. Collins, C. B., Davanloo, F., Dussart, R., Iosif, M. C., Hicks, J. M., Karamian, S. A., Ur, C. A., Popescu, I. I., Kirischuk, V. I., Carroll, J. J., Roberts, H. E., Mc Daniel, P. and Crist, C. E., *Phys. Rev. Lett.* **82** (1999), 695.
25. Collins, C. B., Davanloo, F., Rusu, A. C., Iosif, M. C., Zoita, N. C., Camase, D. T., Hicks, J. M., Karamian, S. A., Ur, C. A., Popescu, I. I., Dussart, R., Pouvesle, J. M., Kirischuk, V. I., Strilchuk, N. V., Mc Daniel, P. and Crist, C. E., *Phys. Rev. C* **61** (2000), 054305.
26. Collins, C. B., Zoita, N. C., Rusu, A. C., Iosif, M. C., Camase, D. T., Davanloo, F., Emura, S., Uruga, T., Dussart, R., Pouvesle, J. M., Ur, C. A., Popescu, I. I., Kirischuk, V. I., Strilchuk, N. V. and Agee, F. J. (submitted).